Lab on a Chip

TECHNICAL INNOVATION

View Article Online
View Journal | View Issue

Cite this: *Lab Chip*, 2014, **14**, 1673

A microfluidic tubing method and its application for controlled synthesis of polymeric nanoparticles†

Jidong Wang,‡[a] Wenwen Chen,‡[a] Jiashu Sun,*[a] Chao Liu,[b] Qifang Yin,[b] Lu Zhang,[a] Yunlei Xianyu,[a] Xinghua Shi,[b] Guoqing Hu*[b] and Xingyu Jiang*[a]

Received 18th January 2014,
Accepted 17th February 2014

DOI: 10.1039/c4lc00080c

www.rsc.org/loc

This report describes a straightforward but robust tubing method for connecting polydimethylsiloxane (PDMS) microfluidic devices to external equipment. The interconnection is irreversible and can sustain a pressure of up to 4.5 MPa that is characterized experimentally and theoretically. To demonstrate applications of this high-pressure tubing technique, we fabricate a semicircular microfluidic channel to implement a high-throughput, size-controlled synthesis of poly(lactic-*co*-glycolic acid) (PLGA) nanoparticles ranging from 55 to 135 nm in diameter. This microfluidic device allows for a total flow rate of 410 mL h^{-1}, resulting in enhanced convective mixing which can be utilized to precipitate small size nanoparticles with a good dispersion. We expect that this tubing technique would be widely used in microfluidic chips for nanoparticle synthesis, cell manipulation, and potentially nanofluidic applications.

Microfluidic systems are emerging as important tools for chemical and biological applications such as diagnostics and screening.[1–4] Since the invention of microfluidic technologies, polydimethylsiloxane (PDMS) has become one of the most used materials.[5] PDMS-based microfluidic devices provide many benefits, including rapid prototyping, low cost, optical transparency, and easy bonding to different substrates.[6,7] To commercialize these microfluidic systems, most devices require a reliable packaging method. One of the major challenges for packaging is to establish multiple fluidic interconnections from chips to the macroscopic world.[8]

There are basically three kinds of approaches to make interconnections: 1) directly insert tubes into the ports of the chip, 2) glue connectors, such as tubes, tips or capillaries, on the chip surface above the ports, and 3) use rubber O-rings, screws or port clamps to create press-fit connections.[9,10] The first two methods are simple and straightforward, but suffer from some drawbacks, such as fluid leakage from the interconnection at a high-pressure, channel clogging by adhesives, and a large dead volume.[7] The press-fit interconnections always require additional components, such as holders and clamps, and a lack of flexible adoption.[11,12] Recently, many efforts have been made to design and fabricate standardized, plug-and-play, and multichannel interfaces for microfluidic devices.[8,10,13] One aim of these chip-to-world interfaces is to automatically introduce different reagents and samples into microfluidic devices for chemical or biological analyses.[2]

Since most microfluidic systems take advantage of small length scales and low Reynolds numbers, the interconnections only need to sustain a pressure of several atmospheres.[10] Typically, press-fit connections can support a maximum pressure of around 1.5 MPa.[14] A glued tubing interconnection can sustain an inlet pressure of 600 kPa.[6] Nevertheless, a high-pressure or high-velocity operation inside microfluidic devices would lead to unique flow phenomena and can induce additional benefits, thus endowing microfluidics with new characteristics. In our previous studies, we demonstrated a rapid and continuous tumor cell separation from blood cells based on a hydrodynamic inertial effect that manifests only at a relatively high velocity.[15,16] In addition, microfluidic-based reactions under high-pressure may significantly increase the rates of thermal and mass transfer, thus enabling aggressive reaction conditions and high-throughput production. For example, a high inlet flow pressure and high-pressure capacity of the tubing interconnection are required to increase the yield of nanoparticles synthesized in microfluidic platforms.

Here, we present a simple and flexible tubing method to connect PDMS chips to external equipment such as syringe pumps. Microfluidic channels are fabricated using standard soft-lithography techniques with an SU8 master mold on a silicon substrate.[4] The microfluidic chip for leakage tests has

[a] *Beijing Engineering Research Center for BioNanotechnology & Key Lab for Biological Effects of Nanomaterials and Nanosafety, National Center for NanoScience and Technology, Beijing, 100190, China.*
E-mail: xingyujiang@nanoctr.cn, sunjs@nanoctr.cn
[b] *Institute of Mechanics, Chinese Academy of Sciences, 100190, China.*
E-mail: guoqing.hu@imech.ac.cn

† Electronic supplementary information (ESI) available. See DOI: 10.1039/c4lc00080c

‡ These authors contributed equally to this work.

a straight channel which is 50 μm wide (or 300 μm wide), 50 μm deep, and 6 cm long (Fig. 1a). The semicircular channel for preparing the nanoparticles is 300 μm wide, 50 μm deep and has a total length of 5 cm (Fig. S4†). Degassed PDMS (mixed in a 10 : 1 ratio of PDMS base to curing agent, Sylgard 184, Dow Corning Inc.) is poured over the mold, and baked at 80 °C for 2 h in an oven. The PDMS slab has a thickness of around 5 mm, which is removed from the silicon substrate with a razor blade (Fig. 1a).

After obtaining the PDMS slab, we use a flat-tipped needle (the inner diameter of the needle is 0.5 mm and the outer diameter is 0.8 mm) with a sharpened outer edge to carefully punch a hole of 0.5 mm in diameter in the channel inlet. We place the PDMS chip in a new Petri dish, and gently press it down to ensure complete contact between the embedded microchannel and the dish surface.

Before inserting a plastic tube (inner diameter of 0.5 mm, outer diameter of 1 mm) into the hole, we smear a small amount of adhesive sealant (Dow Corning® 3145 RTV) 2 mm above the beveled end of the tube (Fig. 1b and S1†). To secure this tubing interconnection, we pour another layer of uncured PDMS on top of the PDMS chip to totally cover the interconnection, and bake the whole device inside the Petri dish at 80 °C for 2 h. The thickness of this two-layer PDMS device is 8 mm. The assembled PDMS chip with the tubing is finally bonded to a glass slide *via* plasma treatment (Fig. 2). Although we use an adhesive in our tubing system, no clogging of the microchannels and no sealant contamination occurs because: 1) the smeared adhesive is above the beveled end of the tube before inserting the tube into the PDMS port (Fig. S1†); 2) the adhesive will remain on the PDMS surface after inserting the tube into the port as the diameter of the soft PDMS port is smaller than that of the rigid tube (Fig. S1†); 3) the adhesive used here is a non-flowing adhesive with high tensile strength that won't flow through the small gap between the plastic tube and the PDMS port during solidification.

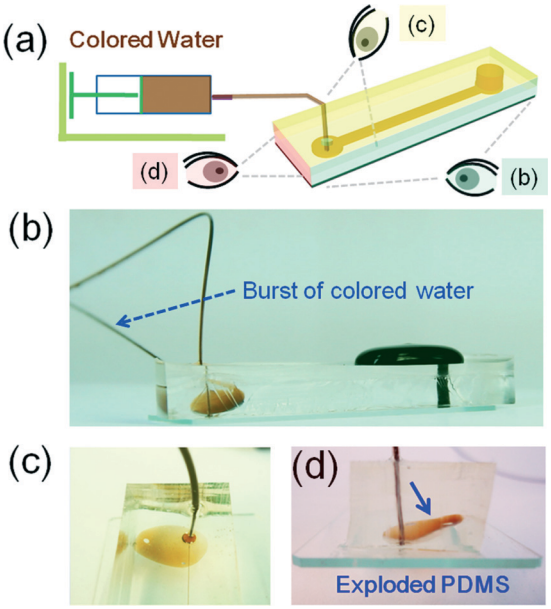

Fig. 2 Leakage tests of the tubing interconnection for the straight microchannel. (a) A schematic of the experimental set-up. The microfluidic channel is connected to a syringe pump through the tubing interconnection. (b) A snapshot of colored water bursting at the inlet interconnection of the microchannel (300 μm wide × 50 μm high × 6 cm long) at 800 mL h^{-1}. (c) and (d) show photographs of the tubing interconnection after the leakage at different camera angles. The small arrow indicates the interstice of the exploded PDMS.

To characterize the ability of this tubing interconnection to withstand pressure, we perform a leakage test. After fabrication of the interconnection, a syringe pump (PHD Ultra, Harvard Apparatus) is applied to infuse colored water through a 5 mL syringe into the microfluidic channel (50 μm × 50 μm cross-section). The flow rates can be adjusted by the syringe pump, and we use six flow rates (10 mL h^{-1}, 20 mL h^{-1}, 30 mL h^{-1}, 40 mL h^{-1}, 50 mL h^{-1} and 60 mL h^{-1}) to characterize the

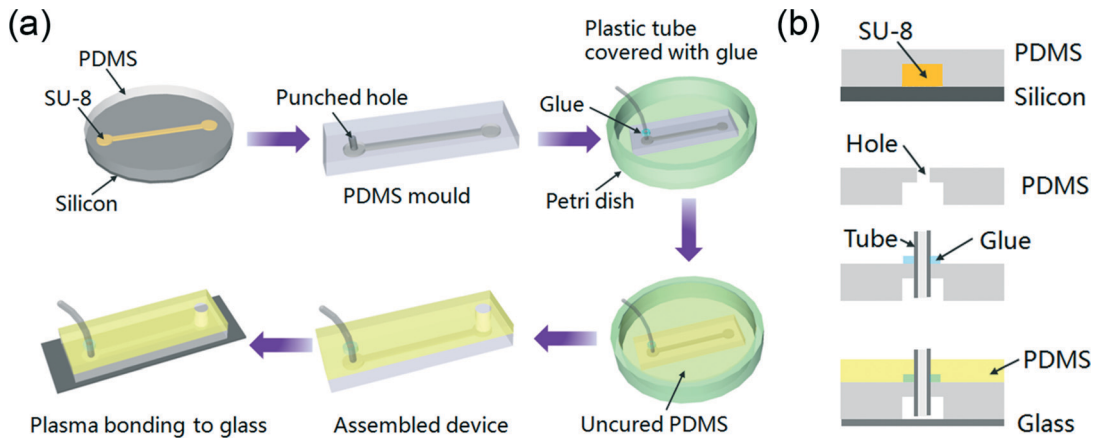

Fig. 1 Schematics of fabricating a tubing interconnection for PDMS microfluidic devices. (a) A PDMS chip with a cored port is placed in a new Petri dish, followed by inserting a plastic tube covered with a small amount of glue at the end. An uncured layer of PDMS is poured on top of the PDMS chip, and baked to solidify. The assembled PDMS chip with the tubing is bonded to a glass slide by plasma treatment. (b) A cross-sectional illustration of the tubing interconnection fabrication. The fabrication process of the tubing interconnection for both the straight and the semicircular microchannel is the same.

performance of the interconnection. Each flow rate is kept constant until 5 mL water has run out or the interconnection bursts. Six microfluidic chips with the same dimensions are made for repeat experiments. We also fabricate another straight microchannel that is 300 μm wide, 50 μm high, and 6 cm long to test the burst pressure of the interconnection. The burst process is recorded by a digital camera (Nikon) for the straight channel.

Because PDMS is an elastic material, a high flow rate will lead to channel deformation, thus affecting the pressure drop and flow profile inside the channel. The tendency of channel deformation increases with decreasing the aspect ratio of the microchannel (height/width).[17] To characterize the performance of the tubing interconnection, we use a straight channel (6 cm long) with a square cross-section of 50 μm × 50 μm to minimize the effect of channel deformation. The hydraulic resistance (R_{hyd}) for the straight channel with the square cross-sectional shape is given by:[18]

$$R_{hyd} = 28.4\eta L\frac{1}{h^4} \quad (1)$$

where η is the viscosity of the fluid, L and h are the length and height of the microchannel, respectively. The hydraulic resistance of our channel is 2.73×10^{14} Pa s m^{-3}. The pressure drop (Δp) across this channel at a constant flow rate (Q) is:

$$\Delta p = R_{hyd}Q \quad (2)$$

When we use a syringe pump to constantly inject colored water into the microchannel, the pressure at the interconnection can be calculated by eqn (2). Up to a flow rate of 50 mL h^{-1} (Re = 278), there is no leakage from the tubing interconnection or the bonding interface for 6 min. However, if we increase the flow rate to 60 mL h^{-1} (Re = 333), the tubing interconnection bursts within a minute. This flow rate will impose a pressure of 4.5 MPa on the inlet, which is also confirmed by a numerical simulation (Fig. S2†).

Unlike most chips where the leakage is either at the tubing interface or the bonding interface between PDMS and the glass, the burst of our interconnection is at the interior of PDMS under a high-pressure (Fig. 2). We make six microfluidic channels (50 μm wide × 50 μm high × 6 cm long) using the same tubing technique for testing purposes, and all of them burst at 60 mL h^{-1}. We also note that the explosion of PDMS takes place around the inlet PDMS port, and results in a tilted crack (Fig. 2). For comparison, we make a glued tubing interconnection without the second layer of PDMS for the same microchannel, and perform the leakage test. The experimental observation indicates that the colored water leaks from the gap between the plastic tube and the PDMS port at a low flow rate of 10 mL h^{-1}, corresponding to an imposed pressure of 0.75 MPa (Fig. S3†).

Another straight microfluidic channel of 300 μm width, 50 μm height, and 6 cm length is used to test the pressure capability of our tubing interconnection. The hydraulic resistance ($R_{hyd,r}$) for the straight channel with a rectangular cross section is:[18]

$$R_{hyd,r} = \frac{12\eta L}{1-0.63(h/w)}\frac{1}{h^3 w} \quad (3)$$

where w is the width of the microchannel. By using this equation, we can obtain a channel resistance of 2.15×10^{13} Pa s m^{-3}. This interconnection can support an inlet flow rate of 750 mL h^{-1} for 1 min, and bursts at the interior of PDMS as we increase the flow rate to 800 mL h^{-1}, yielding an inlet pressure of 4.77 MPa (Fig. 2 and movie S1 at the top, in the ESI†). We also fabricate a simple glued interconnection for this channel, which leaks at 150 mL h^{-1}, corresponding to a pressure of 0.9 MPa (movie S1 at the bottom, in the ESI†). To expand the current pressure limit of our two-layered tubing system, other materials like Teflon with better mechanical properties should be used to fabricate microfluidic chips.

Nanoprecipitation is a simple and widely used method to prepare nanoparticles. This method typically uses water-miscible solvents to dissolve a polymer, and dips the polymer solution slowly into water using sonication or stirring. The interfacial deposition of polymeric nanoparticles occurs as soon as the solvent mixes with water. Therefore, rapid and sufficient mixing is vital to generate small-sized and well-dispersed nanoparticles.[19] Microfluidic-based nanoprecipitation enables the precise control of mixing on a small length scale, thus becoming a promising platform for the controlled synthesis of nanoparticles.[20] A major challenge for microfluidic-based synthesis, however, lies in the low productivity of nanoparticles, which is limited by the low flow rate ranging from hundreds of μL to several mL per hour inside microfluidic devices. With our tubing interconnection technique, we can dramatically increase the productivity by increasing the flow rates of the polymer solution and water (Fig. S4†).

We first investigate the mixing at a low flow rate with different flow rate ratios (FRs) inside the three-inlet semicircular microchannel of 300 μm width × 50 μm height × 5 cm length. The middle fluorescein stream at 1 to 4 mL h^{-1} is hydrodynamically focused into a narrow band by two water sheaths of 20 mL h^{-1} each, which is confirmed by a three-dimensional (3D) model using Fluent (Fig. S5 and S6†). The width of the focused stream becomes wider when increasing the flow rate of the middle stream, indicated by a reduced FR from 40 to 10 (Fig. S6†). At a total flow rate of 41 to 44 mL h^{-1}, the Reynolds number inside the microchannel is around 65, and the mixing mainly relies on diffusion. In comparison, by employing our tubing method, we can significantly increase the total flow rate ten times to 410 mL h^{-1} (Re = 650). The inlet pressure is estimated to be 4.2 MPa by using a numerical simulation. With a significant increase of the Reynolds number inside the semicircular microchannel, four micro-vortices perpendicular to the flow direction are generated at the junction of the three inlets due to the stronger Dean flow, resulting in more efficient convective mixing at a FR of 10 to 40 (Fig. S6 and S7†). The 3D confocal images also confirm

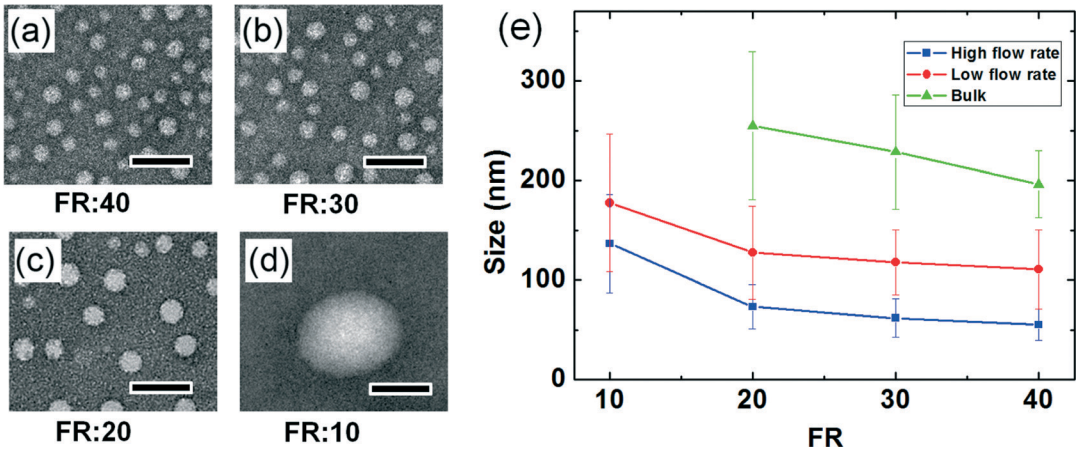

Fig. 3 TEM images of PLGA nanoparticles precipitated under different FRs. (a) Middle channel: 10 mL h^{-1}, each side channel: 200 mL h^{-1}, and FR: 40, (b) middle channel: 13 mL h^{-1}, each side channel: 198.5 mL h^{-1}, and FR: 30, (c) middle channel: 20 mL h^{-1}, each side channel: 195 mL h^{-1}, and FR: 20, and (d) middle channel: 38 mL h^{-1}, each side channel: 186 mL h^{-1}, and FR: 10. The scale bar is 100 nm. (e) Size distribution of PLGA nanoparticles as a function of FR using different approaches.

that at a low Re number, diffusional mixing has a constant profile in the *z* direction after the three streams enter the main channel (Fig. S5†). In comparison, convective mixing at a high Re number results in chaotic mixing in the *z* direction, which occurs at the junction of the three inlet streams (Fig. S5†).

Based on the above investigation, we synthesize PLGA nanoparticles at low and high flow rates with varying FRs (ESI†). PLGA nanoparticles of a small size of approximately 55 nm are obtained at a high flow rate (410 mL h^{-1}, Re = 650) and a large FR (40). The sizes of the nanoparticles increase to around 70 nm by adjusting the FR to 20. When we further decrease the FR to 10, a larger size of approximately 135 nm is achieved (Fig. 3). Both TEM and DLS results indicate a good dispersion of PLGA nanoparticles (Fig. 3). We also characterize PLGA nanoparticles synthesized at a low flow rate (41 to 44 mL h^{-1}, Re = 65) with a FR of 10 to 40. The sizes of the nanoparticles are 110 nm at a FR of 40, and increase to 180 nm at a FR of 10 (Fig. 3). At the same FR, the nanoparticles obtained at a high flow rate (410 mL h^{-1}) are approximately 50 nm smaller than those at a low flow rate (41 to 44 mL h^{-1}) (Table 1). We speculate that this size difference is caused by diffusion mixing *versus* convective mixing. The convective mixing enables a more efficient and rapid interfacial deposition of small-sized PLGA nanoparticles. In addition, high flow rate synthesis produces nanoparticles with a narrow size distribution and a low polydispersity (PDI) of 0.1, while nanoparticles prepared by low flow rate synthesis have a higher PDI of around 0.2.

Table 1 The comparison of precipitated PLGA nanoparticles using microfluidic (high and low flow rates) and bulk methods

	Total flow rate (mL h^{-1})	Mass production (g h^{-1})	Minimum size (nm)	PDI
Microfluidics	41–44	0.02–0.08	110	~0.2
Microfluidics	410	0.2–0.8	55	~0.1
Bulk		0.1–0.4	200	~0.4

In addition, we precipitate PLGA nanoparticles using a conventional bulk method as follows: 2% PLGA organic solutions (250, 500, 750, and 1000 μL) are added dropwise into four flasks containing 10 mL water, and stirred magnetically for 3 min at room temperature. The mass concentrations of the PLGA nanoparticles are equal to those using the microfluidic approach with FRs between 40 and 10. When adding 1000 μL of the 2% PLGA solution to 10 mL water, visible white PLGA particles precipitate, which exceed the size limits of the DLS measurements. The DLS results of the other three samples indicate that PLGA nanoparticles using the bulk method exhibit large sizes (200–250 nm) and a wide distribution (PDI ~ 0.4) (Fig. 3 and Table 1). The mass production of PLGA nanoparticles using the bulk method ranges from 0.1 to 0.4 g h^{-1}, which is 2 times lower than the high flow rate microfluidic method (Table 1).

Acknowledgements

X. J. and J. S. acknowledge financial support from MOST (2011CB933201, 2012AA030308, 2012AA022703 and 2013AA032204), NSFC (51105086, 91213305, 21025520, and 51073045), and the Chinese Academy of Sciences and Beijing Municipal Science & Technology Commission (Z131100002713024).

Notes and references

1 Y. Y. Liu, Y. Sun, K. Sun, L. S. Song and X. Y. Jiang, *J. Mater. Chem.*, 2010, **20**, 7305–7311.
2 X. Mu, W. F. Zheng, J. S. Sun, W. Zhang and X. Y. Jiang, *Small*, 2013, **9**, 9–21.
3 J. Sun, Y. Kang, E. Boczko and X. Jiang, *Electrochemistry*, 2013, **25**, 1023–1028.
4 J. Sun, C. C. Stowers, E. M. Boczko and D. Li, *Lab Chip*, 2010, **10**, 2986–2993.

5 E. Sollier, C. Murray, P. Maoddi and D. Di Carlo, *Lab Chip*, 2011, **11**, 3752–3765.
6 A. M. Christensen, D. A. Chang-Yen and B. K. Gale, *J. Micromech. Microeng.*, 2005, **15**, 928–934.
7 C. K. Fredrickson and Z. H. Fan, *Lab Chip*, 2004, **4**, 526–533.
8 E. Wilhelm, C. Neumann, T. Duttenhofer, L. Pires and B. E. Rapp, *Lab Chip*, 2013, **13**, 4343–4351.
9 S. Haeberle and R. Zengerle, *Lab Chip*, 2007, **7**, 1094–1110.
10 A. Scott, A. K. Au, E. Vinckenbosch and A. Folch, *Lab Chip*, 2013, **13**, 2036–2039.
11 H. Kortmann, L. M. Blank and A. Schmid, *Lab Chip*, 2009, **9**, 1455–1460.
12 A. Arora, G. Simone, G. B. Salieb-Beugelaar, J. T. Kim and A. Manz, *Anal. Chem.*, 2010, **82**, 4830–4847.
13 A. Chen and T. R. Pan, *Lab Chip*, 2011, **11**, 727–732.
14 A. A. S. Bhagat, P. Jothimuthu, A. Pais and I. Papautsky, *J. Micromech. Microeng.*, 2007, **17**, 42–49.
15 J. S. Sun, C. Liu, M. M. Li, J. D. Wang, Y. L. Xianyu, G. Q. Hu and X. Y. Jiang, *Biomicrofluidics*, 2013, **7**, 011802.
16 J. Sun, M. Li, C. Liu, Y. Zhang, D. Liu, W. Liu, G. Hu and X. Jiang, *Lab Chip*, 2012, **12**, 3952–3960.
17 T. Gervais, J. El-Ali, A. Gunther and K. F. Jensen, *Lab Chip*, 2006, **6**, 500–507.
18 B. Kirby, *Micro- and nanoscale fluid mechanics : transport in microfluidic devices*, Cambridge University Press, New York, 2010.
19 J. Sun, Y. Xianyu, M. Li, W. Liu, L. Zhang, D. Liu, C. Liu, G. Hu and X. Jiang, *Nanoscale*, 2013, **5**, 5262–5265.
20 R. Karnik, F. Gu, P. Basto, C. Cannizzaro, L. Dean, W. Kyei-Manu, R. Langer and O. C. Farokhzad, *Nano Lett.*, 2008, **8**, 2906–2912.